Phase transitions and magnetic properties of $LuFe_2O_4$ under pressure

V. Markovich,[1,*] I. Fita,[2] A. Wisniewski,[2] R. Puzniak,[2] C. Martin,[3] G. Jung,[1,2] and G. Gorodetsky[1]

[1]*Department of Physics, Ben-Gurion University of the Negev, 84105 Beer-Sheva, Israel*

[2]*Institute of Physics, Polish Academy of Sciences, PL-02668 Warsaw, Poland*

[3]*Laboratoire de Cristallographie et Sciences des Matériaux (CRISMAT), UMR 6508, ISMRA, 14050 Caen Cedex, France*

(Received 19 March 2017; revised manuscript received 15 June 2017; published 11 August 2017)

The effect of hydrostatic pressure on complex magnetic phase diagram of $LuFe_2O_4$ has been investigated by various magnetic measurements in the range of 0–12 kbar. The temperature of the ferrimagnetic (fM) transition ($T_N \approx 245$ K) practically does not change with increasing pressure, while the temperature of the appearance of mixed fM and antiferromagnetic (AFM) state at ~ 200 K increases with the rate $dT_C/dP \approx 0.8$ K/kbar. Moreover, an applied pressure suppresses the magnetization, enhances the field of metamagnetic transition, and extends the range of existence of mixed fM and AFM state. Suppression of the ordered magnetic moment under pressure induces a transition from a counterclockwise (CCW) thermal hysteresis below $T \approx 220$ K to a clockwise (CW) thermal hysteresis in a magnetic field $H = 1$ kOe. Nevertheless, field induced metamagnetic transition from mixed fM and AFM state to fM state results in a narrowing of the temperature range of thermal hysteresis and in restoring of CCW type of thermal hysteresis. As a consequence of metamagnetic transition, the thermal hysteresis completed at $H = 10$ kOe remains one of the CCW type under applied pressure.

DOI: 10.1103/PhysRevB.96.054416

I. INTRODUCTION

In recent years, considerable interest has been devoted to studies of multiferroic materials, owing to their potential applications such as memory and spintronics devices [1,2]. A special group of multiferroics represent materials in which ferroelectricity is caused by the Fe^{2+} and Fe^{3+} charge ordering (CO). A prominent example of a frustrated charge ordered system is the $LuFe_2O_4$ (LFO) compound with CO temperature $T_{CO} \sim 330-340$ K [3,4]. This compound exhibits a complex magnetic structure and a plethora of magnetic and structural transitions occurring below T_{CO}. However, there are significant differences between various published reports considering not only the values of the critical temperatures but even the very nature of magnetic structure and the type of coexisting phases in LFO. Moreover, recent studies of the dielectric permittivity cast doubt on the ferroelectric nature of the ac dielectric response in LFO and suggest that the colossal dielectric constant is an artifact appearing due to the capacitance of the surface or the electrical contacts [5–7].

Ikeda *et al.* [8,9] demonstrated that electronic ferroelectricity in LFO originates from the charge valence order of Fe^{2+} and Fe^{3+} ions instead of cation displacements, which starts to appear at temperatures above the ferrimagnetic (fM) ordering temperature at $T_N \approx 240$ K. Detailed x-ray and neutron scattering studies [10–12] have shown that below T_N a complex magnetic ground state appears. Indeed, results of dc magnetization and ac susceptibility measurements of LFO single crystals have revealed below T_N additional magnetic and structural transitions at 225 K and 170 K, separating different cluster glass (CG) states, and a kinetically arrested state (for which the kinetics of the first order transition is arrested, preserving the high-temperature structure while avoiding the first order liquid-crystal transition) below 55 K [13–15]. The kinetically arrested glassy state at $T < 55$ K was studied by analysis of the Arrott plot for magnetization and magnetocaloric effect [13], confirming that the system becomes fully frozen when the applied magnetic field exceeds a critical value of about 45 kOe. Phan *et al.* [13] also suggested that the origin of giant magnetic coercivity at low temperatures (LTs) in LFO should be attributed to the collective freezing of fM clusters and to the enhanced domain wall pinning associated with a structural transition at 170 K. The frustrated triangular topology of the Fe lattice is likely to represent a significant ingredient of the complex physical phenomena observed for LFO, which affects both the charge and the spin orderings [3,4,10,11].

External pressure (P) is a fundamental thermodynamic variable, which affects both the volume of the unit cell and the local structure, which may substantially modify the magnetic and structural properties of studied system. Thus, studies under high pressure may give further information on the interplay between the structure and magnetism. For rare-earth ferrites, pressure investigation, up to 6 kbar, were pursued for YFe_2O_4 and $ErFe_2O_4$, exhibiting two successive magnetic transitions in the temperature range 200–250 K [16,17]. It was found that pressure dependences of the magnetic phase transitions are quite different, despite similar crystal structures. In particular, the higher transition temperature decreases with increasing pressure for YFe_2O_4, while it increases in the $ErFe_2O_4$ case. The lower transition temperature decreases with applied pressure in both compounds, but transition disappears in YFe_2O_4 under the modest pressure of 6 kbar. Recently, a study of the pressure effects, up to $P = 25$ kbar, on the ac susceptibility and resistivity of LFO has shown that T_N decreases with increasing pressure with the rate $dT_N/dP = -0.4-0.5$ K/kbar, indicating that pressure favors a paramagnetic state and suppresses a fM one [18]. On the other hand, synchrotron x-ray and neutron diffraction experiments [19] at $P \leqslant 30$ kbar have demonstrated that although the crystal structure is nearly rhombohedral at room temperature

*Present address: Department of Physics, Ben-Gurion University of the Negev, P.O. Box 653, 84105 Beer-Sheva, Israel; markoviv@bgu.ac.il

 ©2017 American Physical Society

and at $P = 0$, a monoclinic distortion, which is observed at LTs [20], increases with increasing P. In the magnetically ordered regime, the ordered magnetic moment gradually decreases with increasing pressure and at 50 K decreases by up to 30% at 30 kbar [19]. Makarova *et al.* [19] suggested that this effect is possibly related to the melting of the charge ordered state in the studied pressure range.

It was also reported [21] that LFO exhibits a large exchange bias (EB) effect below 200 K. Yoshii *et al.* [21] suggested that the EB effect appears as a result of ferromagnetic-antiferromagnetic (FM-AFM) competition and magnetic frustration. It was proposed that strong Fe-Fe interactions lead to large magnetic single-ion anisotropy. On the other hand, the enhancement of the coercivity was attributed to the collective freezing of nanoscale pancake-like fM domains with large uniaxial magnetic anisotropy [22]. Although further study of magnetic properties of LFO has shown also huge coercivity at LTs, Sun *et al.* [23] argued that the EB effect is absent in LFO.

In order to clarify contradictory observations regarding magnetic structure and the nature of the magnetic transitions in LFO, we have investigated the effect of an applied hydrostatic pressure on its magnetic properties. In this paper, we report on the measurements of field-cooled (FC) magnetization at cooling (FCC) and warming (FCW), zero-field-cooled (ZFC) magnetization, thermoremanent magnetization (TRM) M_r, ac susceptibility, and magnetization hysteresis loops. Presented results demonstrate that an appearance of mixed FM and AFM state below fM transition temperature, strongly affected by pressure, leads to a rich phase diagram of the studied compound and allows us to explain inconsistent data reported so far.

II. EXPERIMENTAL AND RESULTS

Polycrystalline samples employed in the experiments were prepared via solid state reaction, described in detail elsewhere [11]. Magnetic measurements in magnetic field up to 15 kOe were performed with a PAR 4500 vibrating sample magnetometer, while at higher magnetic fields, the measurements were performed using the ac susceptibility and dc magnetization and vibrating sample magnetometer options of the Quantum Design 9 T Physical Property Measurement System.

For the experiments, we have prepared cylinder shaped samples with 1 mm diameter and 4 mm height. The measurements under hydrostatic pressure were performed in the pressure range up to ~ 12 kbar. A miniature container of CuBe with an inside diameter of 1.4 mm was employed as a pressure cell, and silicon oil was used as a pressure-transmitting medium [24]. The pressure at LT was determined from the well-known dependence of the superconducting transition temperature of pure tin sample on pressure. The tin sensor was placed next to the investigated sample.

Figure 1(a) shows the temperature dependences of the FCC and FCW magnetization of the LFO sample at magnetic field of 200 Oe, under ambient ($P = 0$) and applied pressure of 10.6 kbar. Magnetization measured at $P = 0$ and 10.6 kbar starts to increase sharply below 260 K and exhibits a magnetic transition at $T_N \approx 247$ K. For FCC and FCW magnetization recorded at $P = 0$, a pronounced thermal hysteresis is clearly seen in the wide temperature interval between 70 and 240 K. It is well known (see Fig. 1 in Ref. [25]) that the magnetization

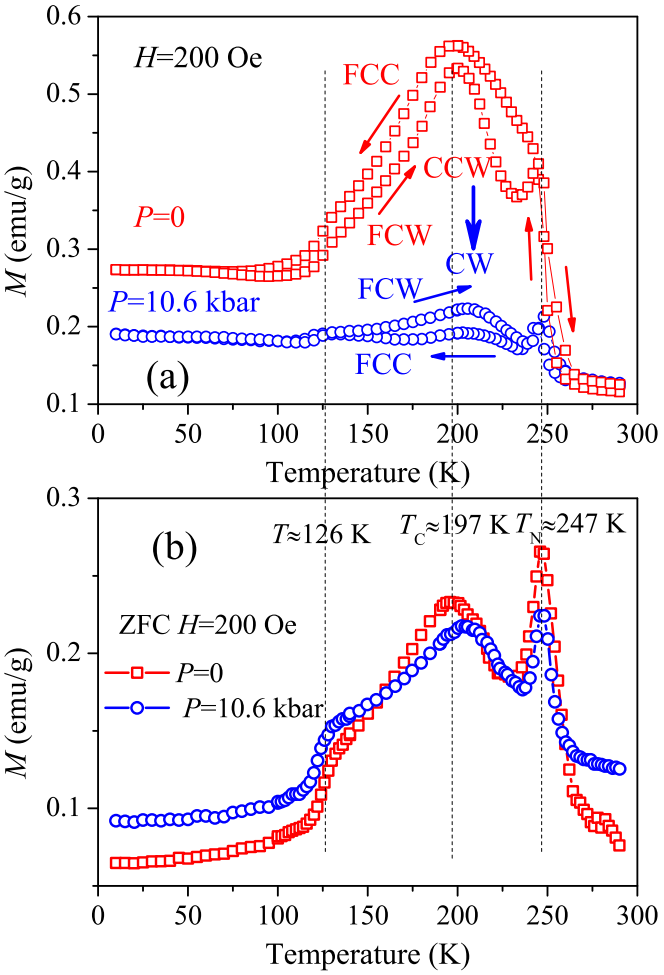

FIG. 1. (a) Temperature dependence of the FCC and FCW magnetization of $LuFe_2O_4$ recorded in magnetic field $H = 200$ Oe at ambient, $P = 0$, and at applied pressure $P = 10.6$ kbar. Arrows show the direction of the temperature change, while the bold solid arrow points to the change of the thermal hysteresis type. (b) Temperature dependence of the ZFC magnetization of $LuFe_2O_4$ recorded in magnetic field $H = 200$ Oe at the ambient pressure and at $P = 10.6$ kbar. Dashed lines mark features related to the magnetic transitions.

below the first order magnetic transition typically exhibits a counterclockwise (CCW) thermal hysteresis, as the one recorded at $P = 0$. It should be noted, however, that some phase separated systems may also exhibit a clockwise (CW) thermal hysteresis [26,27]. It is also well seen that both FCC and FCW magnetization at $P = 0$ exhibit a maximum at temperature close to 197 K. At LTs below 55 K, both the FCC and FCW magnetization curves well coincide. This is considered to be a signature of the kinetically arrested state [26,28].

The temperature evolution of FCC and FCW magnetization measured under pressure at $H = 200$ Oe shows several noticeable features. (i) The magnetic transition temperature (T_N), associated with strong increase of the magnetization, seems to be not affected by the applied pressure. (ii) The FCC and FCW magnetization, measured under pressure $P = 10.6$ kbar, starts to diverge only above ~ 90 K, possibly as a hallmark of the

pressure induced extension of the temperature range in which the kinetically arrested state exists. (iii) Remarkably, a change in the type of thermal hysteresis from a CCW type at $P = 0$ to a CW one at $P = 10.6$ kbar is noticed.

Figure 1(b) shows temperature dependence of the M_{ZFC} recorded at the applied field of 200 Oe under ambient pressure and $P = 10.6$ kbar. The $M_{ZFC}(T)$ curve at $P = 0$ exhibits a sharp peak near T_N. The long-range magnetic ordering in the studied sample occurs at $T_N = 247$ K, in good agreement with $T_N = 240$ K, reported in the literature [10–13]. Christianson *et al.* [12] reported on a transition at 175 K, identified as the magnetostructural transition characterized by the broadening of a number of diffraction peaks and by the growth of a diffuse component in the magnetic scattering data. Nevertheless, $M_{ZFC}(T)$ dependence observed by us is featureless around 175 K, while a broad maximum is clearly seen at $T \approx 197$ K at the ambient pressure.

Recent neutron scattering experiments [11] provide evidence for the complex magnetic ground state and for magnetic ordering in $[Fe_2O_4]_\infty$ bilayers of the LFO. Modeling of the diffraction data pointed to the coexistence of magnetic phases with opposite signs of the intrabilayer interactions and to the appearance of two distinct ordering temperatures: FM bilayers order around 250 K, while AFM bilayers order around 200 K [11]. Consequently, we tentatively identify the temperature $T_C \approx 197$ K with the ordering temperature of AFM bilayers. Data shown in Fig. 1 demonstrate that T_N is practically not sensitive to the applied pressure, while the T_C of the second transition increases under pressure with the rate $dT_C/dP \approx 0.8$ K/kbar.

Figure 2(a) shows the temperature dependence of the FC magnetization of the LFO sample recorded during FCC and FCW cycles at magnetic field of 1 kOe under $P = 0$ and at applied pressure of 11.5 kbar. For the magnetization measured at $H = 1$ kOe under $P = 0$, the $T_N \approx 244$ K was determined from the position of a minimum in the derivative dM_{FCC}/dT (not shown). A pronounced thermal hysteresis is also seen in the wide temperature interval between 70 and 220 K. At LTs below 55 K, both the FCC and FCW magnetization curves coincide well. The temperature evolution of FCC and FCW magnetization measured under pressure also shows additional interesting features: (i) The T_N seems to be not affected by the applied pressure. (ii) Upon application of 11.5 kbar pressure, the M_{FCC} and M_{FCW} of the ordered state decrease by a factor close to three. (iii) The FCC and FCW magnetization measured under pressure $P = 11.5$ kbar start to diverge only above ~ 90 K, in agreement with the measurements in smaller field of 200 Oe [see Fig. 1(a)]. (iv) Similar to the data at $H = 200$ Oe [Fig. 1(a)], a change in the type of thermal hysteresis from CCW type at $P = 0$ to CW one at $P = 11.5$ kbar also appears.

Figure 2(b) shows the temperature dependence of FCC and FCW magnetization measured at higher applied field of 10 kOe, under ambient ($P = 0$) and at applied pressure of 10.6 kbar. Comparing the data shown in Figs. 1 and 2(a) with those of Fig. 2(b), one finds the following. (i) In a marked contrast to the previously published observations [18], again, there is no visible decrease of T_N under application of the hydrostatic pressure. (ii) The M_{FCC} and M_{FCW} of the ordered state decrease only slightly (by about 10–20%) under pressure. Persistence of the magnetization decrease in high

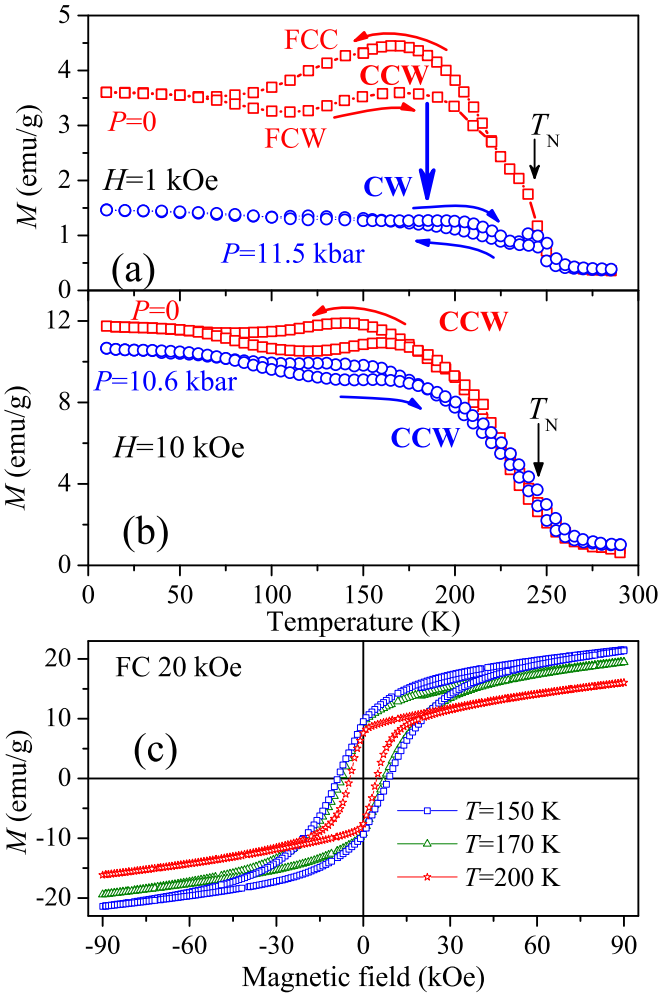

FIG. 2. (a) Temperature dependence of the FCC and FCW magnetization of $LuFe_2O_4$ recorded in magnetic field $H = 1$ kOe at ambient, $P = 0$, and at applied pressure $P = 11.5$ kbar. Arrows show the direction of the temperature change, while the bold solid arrow marks the change of the type of the thermal hysteresis. (b) Temperature dependence of the FCC and FCW magnetization recorded in magnetic field $H = 10$ kOe at ambient, $P = 0$, and at applied pressure $P = 10.6$ kbar. (c) Magnetic field dependence of the magnetization of $LuFe_2O_4$, as measured after FC in magnetic field of 20 kOe at various temperatures for the magnetic field range ±90 kOe.

magnetic fields confirms the decrease of Fe magnetic moment under pressure [19]. (iii) The FCC and FCW magnetization measured under pressure of 10.6 kbar start to diverge at temperatures above ~ 75 K, again indicating the extension of the temperature range of the persistence of the kinetically arrested state under pressure. At the same time, similar to the behavior of the $Nd_{0.5}Sr_{0.5}MnO_3$ system [28], an increase of applied magnetic field by order of magnitude from 1 to 10 kOe does not affect the temperature range in which the kinetically arrested state exists at ambient pressure. However, under applied pressure, the temperature range of the existence of kinetically arrested state expands with increasing magnetic field. (iv) Thermal hysteresis of FCC and FCW magnetization retains its CCW type at a higher field of 10 kOe, independently of applied pressure.

Figure 2(c) shows examples of magnetic hysteresis loops measured in magnetic field up to $H_{max} = \pm 90$ kOe, at some selected temperatures, after FC in $H_{cool} = 20$ kOe. A straightforward noticeable feature of these recordings is the absence of any shifts in the hysteresis loop, indicating the absence of the EB effect in LFO. It is known that the coercive field in LFO grows rapidly with decreasing temperature and approaches 90 kOe at 4 K [22]. Hysteresis loops may properly reveal the presence of the EB effect only when the hysteresis loops are saturated or effectively saturated. In our experiments, this occurs only at temperatures above 150 K. Geshev [29,30] proposed that the presence of a "true" EB in mostly AFM systems in an absence of the saturation may be properly verified by recordings of the effectively saturated hysteresis loops. A system is effectively saturated when the ascending and descending branches of the hysteresis loop coincide at fields higher than the anisotropy field [29,30]. Recently, Harres *et al.* [31] suggested few independent criteria for discrimination between nonsaturated (minor) and saturated (major) or effectively saturated hysteresis loops. Notice that open hysteresis loops (minor loops) presented in Ref. [21] were recorded at $T \leqslant 150$ K and do not fulfill the criteria for the proper observation of the EB effect. Clearly, the effectively saturated loops of the LFO sample, as those shown in Fig. 2(c), do not exhibit any EB effect.

The temperature dependences of the real and imaginary part of magnetic ac susceptibility, χ' and χ'', recorded at the probing field of 10 Oe, are shown in Fig. 3. Sharp peaks are well seen at $T_N = 240$ K in both χ' and χ'' characteristics. The temperature at which the peaks show does not depend on the frequency, but the peak height changes with increasing frequency: The height decreases for χ' and increases for χ''. At temperatures below T_N, the ac susceptibility shows noticeable frequency dependence. Moreover, the temperature dependence of χ' goes through a shallow frequency dependent wide maximum, as seen in the inset of Fig. 3(a), at around 185 K and a pronounced shoulder at around 126 K. The position of the shoulder does not depend on frequency. On the other hand, the maximum in χ'' shifts towards higher temperatures with increasing frequency. The temperature of the maximum at $f = 10$ Hz is close to 126 K and increases to 174 K at $f = 10$ kHz.

The LT feature in $\chi''(T)$ may be associated with freezing of the system into the spin/CG state [32]. The frequency dependence of the peak temperature resembles spin/CG-like behavior and can be characterized by a factor $K = \Delta T_f / T_f \Delta(\log f)$, where T_f is the temperature of the χ'' maximum and ΔT_f is the shift of the temperature of the χ'' maximum for a given frequency difference Δf [32]. The observed frequency shift of the peak's temperature yields the value $K \approx 0.13$ that lies in the range typical for insulating spin glasses. Thus, the evaluated value of the K-factor is in a good agreement with the one obtained from ac susceptibility data of LFO single crystal, for which $K \approx 0.1$ [22].

Observe that ac susceptibility of LFO single crystals [13,22] and polycrystalline samples [18] were studied and analyzed mostly in the context of the spin-glass-like behavior. The temperature dependence of the magnetic susceptibility in a wide temperature range between the room temperature and 4–10 K was presented only in Refs. [13,22]. Some differences

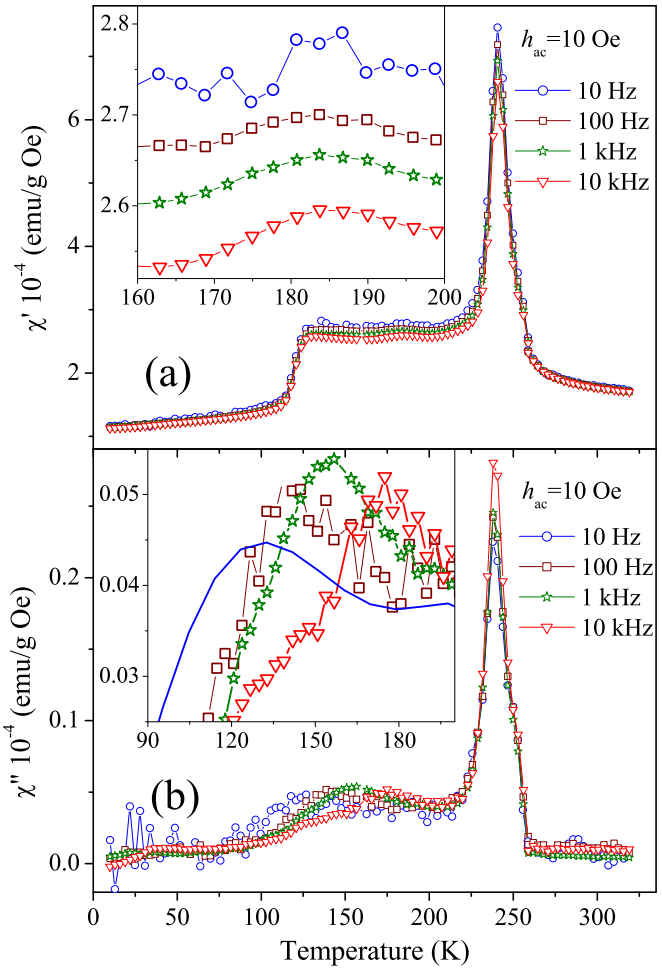

FIG. 3. Temperature dependence of the real (χ') (a) and imaginary (χ'') (b) component of the ac-susceptibility of LFO measured during heating with the ac magnetic field amplitude of 10 Oe at different frequencies. Insets show the behavior of χ' (a) and χ'' (b) around specific features in the temperature dependence. Since 10 Hz data exhibit very large scattering, the experimental results at this frequency are represented by the polynomial line fitted to the data [inset in (b)].

in the magnetization and ac susceptibility data presented by different research groups are likely associated with differences in their samples stoichiometry [4]. The results presented in Fig. 3 are very similar to those shown in Ref. [22] for the LFO single crystal. Wu *et al.* observed an additional dc and ac susceptibility LT feature in the form of a peak or a shoulder at $T_f \approx 80$ K in the static regime [22]. The temperature at which this feature appears strongly increases with increasing frequency from 105 K at $f = 10$ Hz to 140 K at $f = 10$ kHz. Wu *et al.* [22] have related the enhancement of the coercivity observed below T_f to the collective freezing of the nanoscale pancake-shaped fM domains with large uniaxial magnetic anisotropy, which was also visualized by the magnetic force microscopy. By confronting the temperature dependence of magnetization $M_{ZFC}(T)$ from Fig. 1(b) and the ac susceptibility data from Fig. 3 with the results of Wu *et al.* [22], we conclude that the glass transition in the studied polycrystalline sample occurs at $T = 126$ K for $P = 0$ and that the temperature of

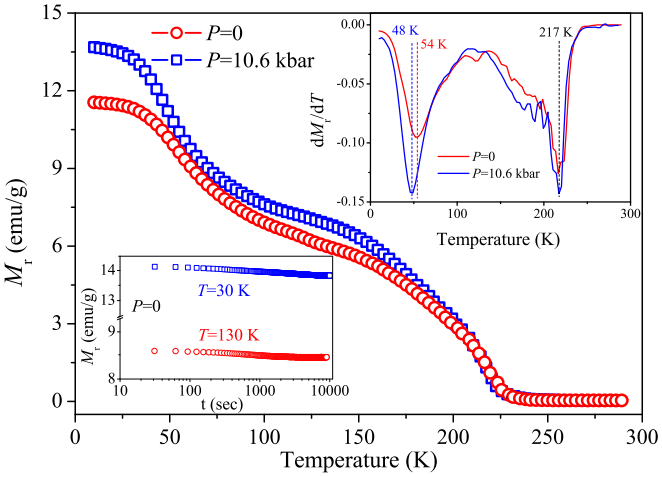

FIG. 4. (a) Temperature dependence of the remanent magnetization M_r of $LuFe_2O_4$ recorded after field cooling in magnetic field $H = 15$ kOe at $P = 0$ and at $P = 10.6$ kbar with the sweep rate of 1.8 K/min. Upper inset shows the temperature dependence of dM_r/dT. The dashed lines indicate positions of the minima of dM_r/dT. Lower inset shows the remanent magnetization of LFO measured as a function of time at $T = 30$ K and $T = 130$ K.

the transition decreases under applied pressure $P = 10.6$ kbar to 122 K. We should, however, observe here that a similar anomaly in the ZFC magnetization at $T \sim 120$ K in LFO was also interpreted as an entrance to the state of the arrested kinetics [14].

Figure 4 shows the temperature dependence of the TRM M_r. The TRM was measured according to the following protocol. The sample was first cooled down to $T = 10$ K in a magnetic field of $H = 15$ kOe. At 10 K, the magnetic field was switched off, and after waiting for 10 s, the temperature dependence of TRM was recorded in the warm-up cycle. The TRM monotonously decreases with increasing temperature and vanishes completely around 230 K. The derivative dM_r/dT exhibits two minima at 48 K and 217 K at $P = 0$ (see upper inset in Fig. 4). The minima are possibly related to the changes in the magnetic state of LFO. The LT minimum shifts up to 54 K under applied pressure of 10.6 kbar, while the high temperature feature is insensitive to the pressure. Phan *et al.* [13] have analyzed the dc magnetization, ac susceptibility, and magnetocaloric data obtained for LFO single crystals and suggested an occurrence of multiple magnetic transitions and glassy states in LFO. They have constructed a complex phase diagram that comprises a paramagnetic to fM transition at around 240 K, followed by the re-entrant CG transition (namely, CG1 state) at ~ 225 K, a second CG transition (namely, CG2 state) below 170 K, and finally an entrance of the kinetically arrested glassy state below 55 K. Confrontation of this phase diagram with reported here $M_r(T)$ dependence allows one to identify the pressure insensitive high temperature feature with the re-entrant CG transition to the CG1 state, with some distribution of fM clusters, while the LT peak marks appearance of the new configuration of fM clusters in the CG2 state that alters the spin dynamics at low temperatures. It follows that the formation of the LT configuration of fM clusters in the CG2 state shifts to higher temperatures under pressure with the rate of 0.5–0.6 K/kbar.

In order to gain further information on the underlying nature of this glassy system, we have measured the relaxation of the remanent magnetization. For the measurements we have employed the following experimental procedure: in TRM protocol, the magnetic field $H = 15$ kOe was applied at room temperature, and the sample was cooled down to the target temperature. Next, the magnetic field was removed and magnetization was immediately recorded. Lower inset in Fig. 4 displays the $M_r(t)$ data recorded at temperatures 30 K and 130 K for $P = 0$. At this temperature range, the time evolution of M_r under an applied pressure is very similar (not shown). The LFO sample exhibits very slow relaxation making the detailed time-dependent studies rather unfeasible. This observation is in general agreement with previous studies of LFO single crystal by Wu *et al.* [22], who found that the system exhibits extremely slow relaxation with the time constants exceeding several days for temperatures below 150 K. They suggested also that at LTs, the increased coercivity can be qualitatively explained by the reduced sensitivity of the collectively frozen state to external perturbations due to increased free energy barriers between the multiple possible states [22]. In particular, in the kinetically arrested glassy state, the barriers are already so large that the relaxation becomes significantly suppressed.

Figures 5(a) and 5(b) show positive field parts of the magnetic hysteresis loops measured after ZFC ($P = 0$) at increasing and decreasing magnetic field up to $H_{max} = 15$ kOe. The form of the hysteresis loops practically does not depend on pressure; therefore, for clarity's sake, we show only the data obtained at ambient pressure. The apparent metamagnetic transition occurring at applied magnetic field is well seen at temperatures near T_N but becomes blurred at lower temperatures. The critical fields of the metamagnetic transition for the up and down field sweep direction are labeled in Figs. 5(c)–5(f) as H_C^+ and H_C^-, respectively. They were determined by the position of the maxima in the derivative dM/dH. The appearance of the hysteresis in the up and down sweep is a hallmark of a phase transition of the first order. With further temperature decrease, the estimation of H_C^- becomes impossible because the transition at decreasing magnetic field is masked by the remanent magnetization appearing below 225 K [see Fig. 4(a)]. The decrease of the critical field with increasing temperature is consistent with the hysteretic metamagnetic transition between the mixed AFM+fM low field phase and the high field fM phase [4,10]. De Groot *et al.* [10] have concluded that the drastic effect of the magnetic field on several reflections in the neutron diffraction patterns and the emergence of an additional intensity on some structural reflections indicate that the step in $M(H)$ corresponds to a coherent effect, i.e., to a genuine metamagnetic transition between AFM and fM spin configurations.

III. DISCUSSION

The values of the critical fields H_C^- and H_C^+ determined in our experiments for the polycrystalline LFO at ambient pressure remain in a good agreement with the critical lines obtained for LFO single crystals from combined

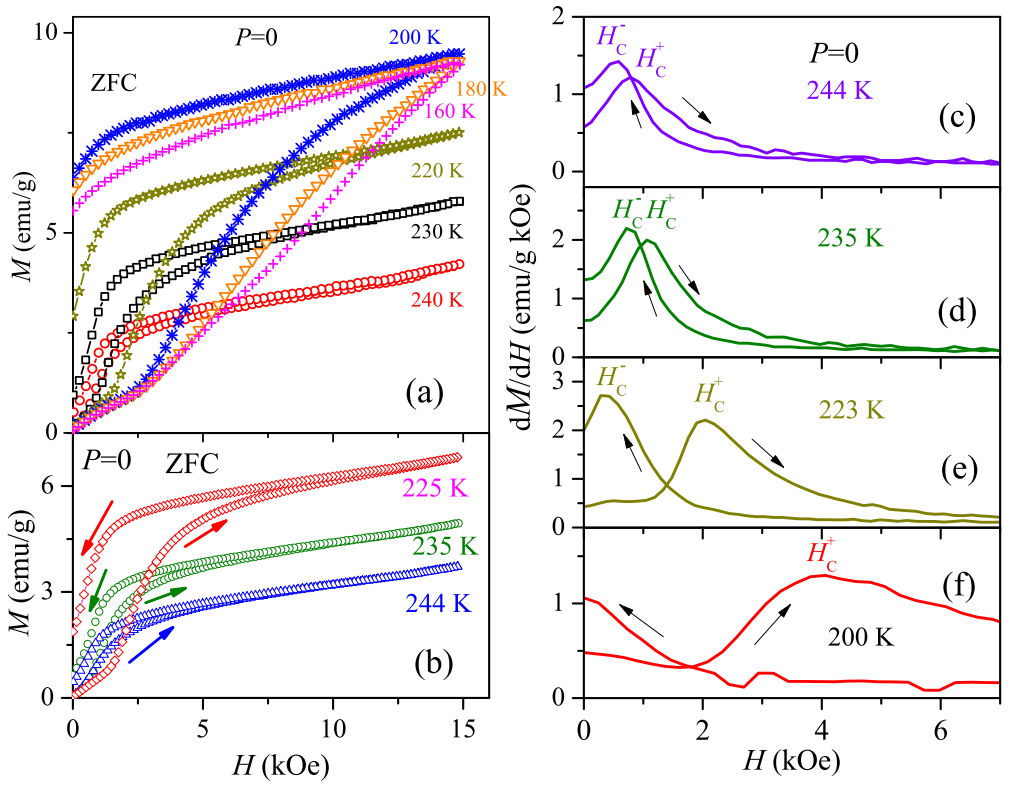

FIG. 5. (a), (b) Magnetic field dependences of the magnetization at various temperatures, as measured after ZFC in increasing and decreasing magnetic field. Arrows show the direction of magnetic field change. (c–f) Magnetic field dependence of dM/dH, measured at $P = 0$. The values of the critical field H_C^+ and H_C^- were determined from the positions of maxima at the up and down field sweeps, respectively.

magnetization, neutron, and soft x-ray diffraction measurements [see Fig. 1(a) in Ref. [10]]. We have used the values of H_C^- and H_C^+ to construct the critical line in the H-T magnetic phase diagram for $P = 0$ and $P = 11$ kbar, as shown in Fig. 6. It can be seen that pressure application increases the

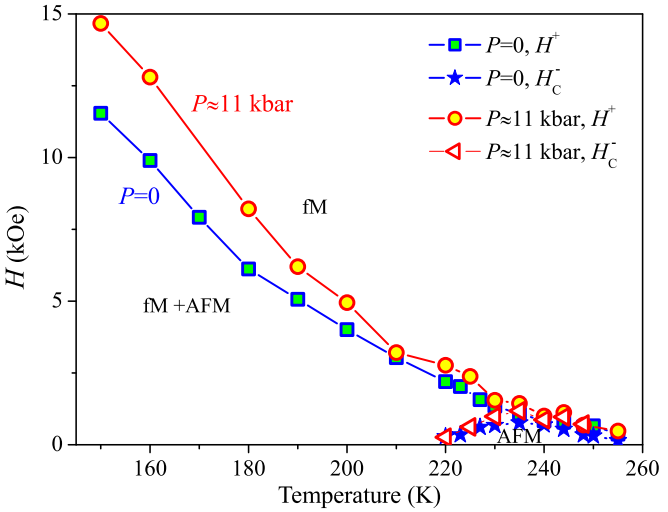

FIG. 6. Critical lines in the magnetic phase diagram constructed using the positions of dM/dH maxima, H_C^+ and H_C^-, measured at up and down field sweeps, respectively. Data under pressure come from two sets of experiments performed under comparable pressures of 10.6 and 11.5 kbar, labeled by $P \approx 11$ kbar.

critical field at $T < 210$ K and thus extends the range of the coexistence of the AFM and fM phase. Let us underline that a complex H-T phase diagram, based on the detailed magnetic, structural, neutron diffraction, optical, and Mössbauer studies, was already presented and discussed in several publications (see Refs. [4,10,13,20]. Here, we just complete it by including the pressure effect on the metamagnetic transition line at the H-T phase diagram.

Various magnetic characteristics measured in our experiments exhibit a relatively sharp magnetic transition at $T_N \approx 240$ K, which can be seen in FCC, FCW, and ZFC measurements (see Figs. 1 and 2). With decreasing temperature, a broader transition appears at around 200 K (see Fig. 1), and then an additional transition is seen as a shoulder in ZFC magnetization and ac susceptibility at around 120 K. The FCC and FCW curves exhibit a pronounced thermal hysteresis, reported earlier by Iida *et al.* [33]. The presence of the hysteresis indicates a first-order magnetic transition or the coexistence of magnetic phases exhibiting nucleation and growth processes [11,33].

Sharp magnetic Bragg reflections have been previously observed in the neutron and soft resonant x-ray diffraction [10] spectra of several LFO single crystals [10,12,15] and polycrystalline samples [11] after cooling below T_N. These peaks are primarily contributed to in the case of the FM bilayer model [11]. Around 200 K, the intensity of some other magnetic peaks, which are predominant in the AFM bilayer model, increases [11]. Bourgeois *et al.* [11] suggested that

such behavior confirms the coexistence of several magnetic phases within the sample at LTs, involving either FM or AFM $[Fe_2O_4]_\infty$ bilayers. Such bilayers can be stacked ferro- or antiferromagnetically and exhibit a spontaneous fM component.

The LT transition near 120 K may be related to the glassy freezing of magnetic moments in the LFO system. In fact, with decreasing temperature, glassy freezing of the magnetically ordered bilayers can be expected to replace the long-range AFM order. Such CG-like behavior, manifested by the frequency dependence in the ac susceptibility, has indeed been previously observed in some LFO samples [13,22]. Alternatively, the possibility of orbital ordering (OO) of the LT phase below 130 K, and its impact on magnetic exchange interactions was considered recently by Angst [4]. Nevertheless, the very nature of the LT phase and its connection with the possible OO in LFO still remains an open question [13].

Some differences appearing in various experiments regarding the magnetic ordering and glassiness of the LFO may be ascribed to differences in oxygen stoichiometry of the employed samples [13,22,34]. Oxygen off-stoichiometry influences the Fe^{2+}/Fe^{3+} ratio and, consequently, the CO. Moreover, the off-stoichiometry destroys the interbilayer spin- and charge-correlations between bilayers and thus leads to a glassy behavior [13,22,34].

The neutron scattering measurements have shown that the magnetic Bragg peaks below $T_N = 240$ K can be indexed in a monoclinic cell, corresponding to the FM or the AFM stacking of the $[Fe_2O_4]_\infty$ bilayers [11,13]. In the AFM or FM arrangement, the configuration within bilayers can be either (↓↑↑↓↑↑) or (↑↓↓↓↑↑), with FM stacking or AFM stacking, respectively [11]. For the fM phase (FM stacking), the net moments of two bilayers of the cell are both ↑, thus resulting in a nonzero sum moment. In the AFM phase, spins of the two nearest bilayers are directed opposite to each other, which results in the AFM ordering [4,11,12]. Close to the T_N, the fM and AFM spin configurations coexist and are almost degenerated at $H = 0$ [10]. The fM and AFM configurations differ only by a flip of all spins in one of the bilayers, which suggests that the spin correlations within the bilayers are much stronger than the interbilayer correlations [4].

Let us discuss briefly the reason of discrepancy between the pressure effect on the transition temperature T_N reported in Ref. [18] and our results. Reported here, magnetization dependences are rather similar to those presented in Ref. [11] for samples with small off-stoichiometry. Indeed, a comparison of Fig. 1 with Fig. 2(a) of Ref. [11] shows that the behavior of the magnetization is similar at $P = 0$, and the magnetization is even somewhat smaller in the studied sample, suggesting that the possible off-stoichiometry is very small. On the other hand, field dependence of the magnetization [see Fig. 1(c)] is very similar to that shown in Fig. 2(b) in Ref. [11], which indicates a similarity of the studied sample and those studied in Ref. [11]. Nevertheless, a smaller value of the magnetization of the studied sample below T_N indicates that it is close to a sufficiently stoichiometric LFO; see, for example, Ref. [10]. On the other hand, ac susceptibility of polycrystalline samples of LFO (presented in Ref. [18]) exhibits only one peak at $T_N = 242$ K in the entire temperature range 77–300 K. This behavior contradicts not only our results but also the behavior of the ac susceptibility of LFO single crystals shown in Refs. [13,22]. A possible reason for such differences may stem from different stoichiometry of the samples studied. In manganite perovskites, a relatively small change in the off-stoichiometry, expressed as vacancies in the cation positions, may cause a significant change in the pressure dependence of the transition temperature [35]. For example, in self-doped $LaMn_{1-x}O_3$, the pressure coefficient dT_N/dP monotonously decreases with increasing x and even changes sign at the modest self-doping $x = 0.06$ [36].

As already noted, the pressure induced enhancement of the monoclinic distortion partially removes the degeneracy between nearly degenerated fM and AFM spin configurations and favors the AFM phase. On the other hand, in the neutron diffraction experiments, magnetic peaks characterizing different magnetic phases of LFO were seen even at the pressure of 30 kbar [19]. Makarova *et al.* [19] proposed that the suppression of the magnetic moment under pressure is related to a progressive destabilization of the charge ordered state under increasing pressure. Recent analysis of the Mössbauer effect spectra confirms that the CO in LFO completely collapses at $P > 30$ kbar [37,38].

Let us discuss the change of type of the thermal hysteresis occurring under pressure in different magnetic fields, clearly seen in Figs. 1(a), 2(a), and 2(b). At the ambient pressure, the width of the thermal hysteresis between FCC and FCW magnetization at around 150 K can be quite large for relatively low applied magnetic field of 1 kOe. The width of the thermal hysteresis changes with the applied hydrostatic pressure and magnetic field. For example, in the applied magnetic field of 1 kOe, the hysteresis width in Fig. 1(a) is close to 150 K at ambient pressure and shrinks to about 70 K after application of the pressure of 11.5 kbar. The pressure enforced reduction of the hysteresis width is much smaller at the higher magnetic field. For the applied field of 10 kOe, the hysteresis width decreases from about 115 K at $P = 0$ to about 100 K at $P = 10.6$ kbar. Surprisingly, however, the type of the hysteresis changes from a CCW to a CW type under application of the hydrostatic pressure at the modest applied field (see Figs. 1 and 2). This unusual behavior should be related to changes in the magnetic structure of the LFO occurring under pressure.

Dantas *et al.* [39] performed theoretical investigations of the magnetization thermal hysteresis for layered structures composed of ferromagnets and helical rare-earth magnets, where the interface coupling is of the AFM and FM type, respectively. They have found that a form of thermal hysteresis (CW or CCW type) in such systems is quite sensitive to even a slight variation of their thickness, as proved by a significant difference in the results obtained for $Fe_{20}/Dy_{10}/Fe_{20}$ and $Fe_{20}/Dy_{12}/Fe_{20}$ trilayers. This is explained by different behavior of magnetic moment for thin and thicker intermediate Dy layer.

The complexity of the LFO magnetic state and the existence of multiple magnetic and structural transitions lead to a situation in which even the very temperatures of the magnetic ordering and spin configurations in the magnetically ordered state of LFO are still under debate in the literature [4,11]. According to the modeling of the magnetic scattering experiments [11], the sign of the intrabilayer coupling actually affects the magnetic ordering temperature since the FM phases order at higher temperature (around 250 K) than the AFM

phases (around 200 K). The modeling of the magnetic ground state at 2 K suggests the presence of four different FM and AFM phases with the following approximate phase ratio: 28(3)% -FM1, 22(3)% -FM2, 32(3)% -AFM1, and 18(3)% -AFM2 [11], indicating that the number of the FM and AFM bilayers in the LFO are roughly equal. It may be concluded that even the definitions for T_C, T_N, and metamagnetic transition between the AFM and fM phases stem from a simplified description of the real system.

In principle, the experimentally observed decrease of the magnetic moment under pressure may be due to two different mechanisms. The first one is the growth of the previously mentioned two AFM phases at the expense of FM phases, while the second one consists of changes in the stacking of the $[Fe_2O_4]_\infty$ bilayers. The enhancement of temperature of the second magnetic transition at ~ 200 K associated with ordering of the AFM phases [11] is an indirect confirmation of the strengthening of AFM phase under pressure. All these effects that occur in a complex magnetic structure may be related to a change of the type of the thermal hysteresis under pressure. The opposite effect of the growth of the FM phases at the expense of AFM phase at high enough magnetic fields results in the growth of the net magnetic moment. This is clearly seen in the magnetic H-T diagram as a transition from the mixed AFM+fM to the fM phase. It may lead to recovering of the thermal hysteresis and to restoring its original CCW type. We suggest that the magnetic structure plays a decisive role in selecting the type of the thermal hysteresis at low magnetic field. Nevertheless, in higher magnetic field $H = 10$ kOe, the structure only weakly depends on the applied pressure, as indicated by a slight magnetization decrease under the pressure and unchanged width of the thermal hysteresis.

In LFO, the LTs monoclinic distortion can be driven by both temperature and magnetic field. The distortion appears below CO transition and becomes well seen below 200 K [20]. Structural and spin degrees of freedom in LFO are linked. The metamagnetic transition from the mixed fM and AFM state to the fM phase in high enough magnetic fields occurs concomitantly with the suppression of the monoclinic distortion [20]. It appears that the applied pressure and magnetic field affect structural distortion in the opposite way, as the monoclinic distortion increases with increasing pressure [19]. Consequently, higher magnetic field should be applied under pressure to induce a metamagnetic transition. This can be seen as well as a clear shift of the H-T line towards higher fields under pressure (see Fig. 6).

IV. CONCLUSIONS

In summary, we have observed several distinct features in the temperature variation of FC magnetization, ZFC magnetization, TRM M_r, and ac susceptibility of LFO and associated them with multiple transitions between different magnetic states and complex magnetic structure. We have found that the ordering temperature T_N is insensitive to the applied pressure, while the temperature of the magnetostructural transition seen at lower temperatures, at around 200 K for $P = 0$, increases with pressure at the rate $dT_C/dP \approx 0.8$ K/kbar, while the temperature of the transition to the CG state at LTs slightly decreases with the applied pressure.

Application of hydrostatic pressure results in suppression of magnetic moment and an enhancement of the metamagnetic transition field in LFO. Suppression of the ordered magnetic moment under pressure can be ascribed to the growth of the AFM phases at the expense of the coexisting FM phases and, presumably, to a change of the stacking of $[Fe_2O_4]_\infty$ bilayers. We have added a pressure dependent critical line to the H-T magnetic phase diagram and demonstrated that the applied pressure extends the temperature range of coexistence of mixed fM and AFM phases. Moreover, for relatively weak applied magnetic field, the applied pressure changes the type of the magnetization thermal hysteresis from the CCW to a CW one. However, at high applied magnetic fields, as a result of the metamagnetic transition from the mixed fM and AFM state to the fM phase, the thermal hysteresis does not change and remains of the CCW type under applied pressure. We have also concluded that properly measured effectively saturated hysteresis loops show no traces of the EB effect in LFO.

Finally, to some readers it may appear that the employed scenario of the coexistence and competition between AFM and fM phases is a rough oversimplification of the complex magnetic nature of LFO. However, we consider it to be only a starting model for studying the complex magnetic and OO in LFO. As noted in a recent review [4], the nature of the magnetic ordering and its relation to the possible OO still remains a major task left for future experimental and theoretical investigations.

ACKNOWLEDGMENTS

This paper was supported by the Polish National Science Centre (NCN) Grants No. 2014/15/B/ST3/03898 and No. 2012/05/B/ST3/03157.

[1] N. A. Spaldin and M. Fiebig, Science **309**, 391 (2005).
[2] W. Eerenstein, N. D. Mathur, and J. F. Scott, Nature (London) **442**, 759 (2006).
[3] M. Angst, R. P. Hermann, A. D. Christianson, M. D. Lumsden, C. Lee, M.-H. Whangbo, J.-W. Kim, P. J. Ryan, S. E. Nagler, W. Tian, R. Jin, B. C. Sales, and D. Mandrus, Phys. Rev. Lett. **101**, 227601 (2008).
[4] M. Angst, Phys. Status Solidi RRL **7**, 383 (2013).
[5] A. Ruff, S. Krohns, F. Schrettle, F. Schrettle, P. Lunkenheimer, and A. Loidl, Eur. Phys. J. B **85**, 290 (2012).
[6] D. Niermann, F. Waschkowski, J. de Groot, M. Angst, and J. Hemberger, Phys. Rev. Lett. **109**, 016405 (2012).
[7] S. Lafuerza, J. García, G. Subías, J. Blasco, K. Conder, and E. Pomjakushina, Phys. Rev. B **88**, 085130 (2013).
[8] N. Ikeda, H. Ohsumi, K. Ohwada, K. Ishii, T. Inami, K. Kakurai, Y. Murakami, K. Yoshii, S. Mori, Y. Horibe, and H. Kito, Nature (London) **436**, 1136 (2005).
[9] N. Ikeda, K. Kohn, N. Myouga, E. Takahashi, H. Kitoh, and S. Takekawa, J. Phys. Soc. Jpn. **69**, 1526 (2000).
[10] J. de Groot, K. Marty, M. D. Lumsden, A. D. Christianson, S. E. Nagler, S. Adiga, W. J. H. Borghols, K. Schmalzl, Z. Yamani, S. R. Bland, R. de Souza, U. Staub, W. Schweika, Y. Su, and M. Angst, Phys. Rev. Lett. **108**, 037206 (2012).
[11] J. Bourgeois, G. Andre, S. Petit, J. Robert, M. Poienar, J.

Rouquette, E. Elkaim, M. Hervieu, A. Maignan, C. Martin, and F. Damay, Phys. Rev. B **86**, 024413 (2012).
[12] A. D. Christianson, M. D. Lumsden, M. Angst, Z. Yamani, W. Tian, R. Jin, E. A. Payzant, S. E. Nagler, B. C. Sales, and D. Mandrus, Phys. Rev. Lett. **100**, 107601 (2008).
[13] M. H. Phan, N. A. Frey, M. Angst, J. de Groot, B. C. Sales, D. G. Mandrus, and H. Srikanth, Solid State Commun. **150**, 341 (2010).
[14] S. Patankar, S. K. Pandey, V. R. Reddy, A. Gupta, A. Banerjee, and P. Chaddah, EPL **90**, 57007 (2010).
[15] A. M. Mulders, M. Bartkowiak, J. R. Hester, E. Pomjakushina, and K. Conder, Phys. Rev. B **84**, 140403(R) (2011).
[16] T. Matsumoto, N. Mori, J. Iida, M. Tanaka, and K. Siratori, J. Phys. Soc. Jpn. **61**, 2916 (1992).
[17] T. Matsumoto, N. Môri, J. Iida, M. Tanaka, K. Siratori, F. Izumi, and H. Asano, Physica B **180-181**, 603 (1992).
[18] X. Shen, C. H. Xu, C. H. Li, Y. Zhang, Q. Zhao, H. X. Yang, Y. Sun, J. Q. Li, C. Q. Jin, and R. C. Yu, Appl. Phys. Lett. **96**, 102909 (2010).
[19] O. L. Makarova, J. Bourgeois, M. Poienar, I. Mirebeau, S. E. Kichanov, G. Andrė, E. Elkaim, M. Hanfland, M. Hervieu, A. Maignan, J. Haines, J. Rouquette, C. Martin, and F. Damay, Appl. Phys. Lett. **103**, 082907 (2013).
[20] X. S. Xu, M. Angst, T. V. Brinzari, R. P. Hermann, J. L. Musfeldt, A. D. Christianson, D. Mandrus, B. C. Sales, S. McGill, J.-W. Kim, and Z. Islam, Phys. Rev. Lett. **101**, 227602 (2008).
[21] K. Yoshii, N. Ikeda, Y. Nishihata, D. Maeda, R. Fukuyama, T. Nagata, J. Kano, T. Kambe, Y. Horibe, and S. Mori, J. Phys. Soc. Jpn. **81**, 033704 (2012).
[22] W. Wu, V. Kiryukhin, H.-J. Noh, K.-T. Ko, J.-H. Park, W. Ratcliff II, P. A. Sharma, N. Harrison, Y. J. Choi, Y. Horibe, S. Lee, S. Park, H. T. Yi, C. L. Zhang, and S.-W. Cheong, Phys. Rev. Lett. **101**, 137203 (2008).
[23] Y. Sun, J.-Z. Cong, Y.-S. Chai, L.-Q. Yan, Y.-L. Zhao, S.-G. Wang, W. Ning, and Y.-H. Zhang, Appl. Phys. Lett. **102**, 172406 (2013).
[24] M. Baran, V. Dyakonov, L. Gladczuk, G. Levchenko, S. Piechota, and H. Szymczak, Physica C **241**, 383 (1995).
[25] Joonghoe Dho, W. S. Kim, and N. H. Hur, Phys. Rev. Lett. **87**, 187201 (2001).
[26] L. Ghivelder and F. Parisi, Phys. Rev. B **71**, 184425 (2005)
[27] A. Banerjee, A. K. Pramanik, Kranti Kumar, and P. Chaddah, J. Phys.: Condens. Matter **18**, L605 (2006).
[28] R. Rawat, K. Mukherjee, Kranti Kumar, A. Banerjee, and P. Chaddah, J. Phys.: Condens. Matter **19**, 256211 (2007).
[29] J. Geshev, J. Appl. Phys. **105**, 066108 (2009).
[30] J. Geshev, J. Phys.: Condens. Matter. **21**, 078001 (2009).
[31] A. Harres, M. Mikhov, V. Skumryev, A. M. H. de Andrade, J. E. Schmidt, and J. Geshev, J. Magn. Magn. Mater. **402**, 76 (2016).
[32] J. A. Mydosh, *Spin-Glasses: An Experimental Introduction* (Taylor and Francis, London, 1993).
[33] J. Iida, Y. Nakagawa, and N. Kimizuka, J. Phys. Soc. Jpn. **55**, 1434 (1986).
[34] F. Wang, J. Kim, G. D. Gu, Y. Lee, S. Bae, and Y. J. Kim, J. Appl. Phys. **113**, 063909 (2013).
[35] V. Markovich, A. Wisniewski, and H. Szymczak, in *Handbook of Magnetic Materials*, edited by K. H. J. Buschow (Elsevier, New York, 2014), Vol. 22, pp. 1–201.
[36] V. Markovich, E. Rozenberg, G. Gorodetsky, G. Jung, I. Fita, R. Puzniak, A. Wisniewski, C. Martin, S. Hebert, and B. Raveau, J. Appl. Phys. **95**, 7112 (2004).
[37] W. N. Sibanda, E. Carleschi, G. Diguet, C. Martin, and G. R. Hearne, in *Proceedings, 59th Annual Conference of the South African Institute of Physics (SAIP 2014)* (Johannesburg, 2014), p. 126.
[38] G. R. Hearne, E. Carleschi, W. N. Sibanda, P. Musyimi, G. Diguet, Yu. B. Kudasov, D. A. Maslov, and A. S. Korshunov, Phys. Rev. B **93**, 105101 (2016).
[39] A. L. Dantas, R. E. Camley, and A. S. Carriço, Phys. Rev. B **75**, 094436 (2007).